Thickness Induced Buckling of bcc Copper Films

B. M. Ocko,[1] I. K. Robinson,[2] M. Weinert,[1] R. J. Randler,[3] and D. M. Kolb[3]
[1]*Department of Physics, Brookhaven National Laboratory, Upton, New York 11973*
[2]*Department of Physics, University of Illinois, Urbana, Illinois 61801*
[3]*Department of Electrochemistry, University of Ulm, D-89069 Ulm, Germany*
(Received 31 March 1999)

Copper films electrodeposited on Au(100) develop a buckling instability after the 11th layer leading to stripes with a 60–75 Å period. Analysis of the x-ray diffraction data shows that the entire copper film restructures by forming regions which are locally orthorhombic in a spatially modulated pattern. This distortion is supported by first-principles calculations.

PACS numbers: 68.55.–a, 81.15.Pq, 81.30.Kf

Face centered cubic (fcc) and body centered cubic (bcc) are common crystallographic arrangements adopted by the elements. Both can be described as body-centered-tetragonal (bct) unit cells with lattice constants a and b equal, but with different special values of the c/a ratio; $c/a = 1$ for bcc and $c/a = \sqrt{2}$ for fcc. Bain suggested that upon biaxial expansion of a and b, and a corresponding relaxation in c/a, a fcc solid may transform continuously into a bcc solid [1]. This would require, assuming volume conservation, a biaxial tensile strain of $2^{1/6} - 1 = 12.2\%$ [2]. A convenient means of introducing such a tetragonal strain is by the pseudomorphic growth of a thin film on a foreign substrate with square symmetry. As its lattice mismatch approaches the necessary 12%, the tetragonal film of an fcc material could thereby become bcc. As we will demonstrate, Cu films up to ten monolayers thick deposited on Au(100) form such a bcc-like phase, but thicker films transform into a uniaxially commensurate, orthorhombic structure with $c/a = 1.18 \pm 0.03$. This thickness induced instability is analogous to the temperature driven martensitic transition observed in other bcc metals such as iron alloys [3].

For Cu, the energy difference between fcc and bcc is quite small, with first-principles calculations giving a value in the range of 7–48 meV/atom depending on the approximations used [4,5]. Contrary to naive expectations, the bulk bcc phase is mechanically unstable [6]; i.e., bcc Cu has soft phonon modes ($\omega^2 < 0$). Combined with the flatness of the energy surface [5,6] around the bcc phase, these features suggest that substrate interactions (favoring commensuration) can easily stabilize surface phases far from either fcc or bcc. For instance, for Cu films on Pd(100) a bct phase is formed with $c/a = 1.12$ over a range of temperature and coverage [7]. For a substrate-stabilized bcc phase of an fcc metal, Bruinsma and Zangwill predicted that at a critical film thickness a martensitic microstructure—twin boundaries—should form as the bcc phase undergoes an orthorhombic distortion [8].

The (100) faces of fcc gold and silver are ideal substrates for investigating the Bain distortion of Cu films. The ratios of their lattice constants ($a_{\mathrm{Au}} = 2.885$ Å, $a_{\mathrm{Ag}} = 2.889$ Å) to that of Cu ($a_{\mathrm{Cu}} = 2.556$ Å) are 1.129 and 1.130, close to the required ratio of 1.122 to form bcc with no volume change [2]. Bruce and Jaeger, on the basis of transmission electron microscopy investigations, proposed that bcc Cu forms for films grown on thin Ag(100) substrates [9] at 600 K. After deposition at 300 K a semiregular pattern of tilted domains appeared with a spacing of about 60–70 Å. Additional information on vacuum deposited Cu on Ag(100) comes from Egelhoff *et al.* [10], who found that the layer-by-layer grown pseudomorphic Cu films are expanded by 4% from the bcc spacing. Studies of Cu electrodeposition on Ag(100) by Dietterle, Will, and Kolb [11] support the vacuum finding of a bcc pseudomorphic growth for films of 8 layers or less. However, with the deposition of the ninth layer, they found a buckled Cu film, attributed to a more compressed top layer.

Under room temperature conditions, where alloying is suppressed, Cu electrodeposition on Au(100) [12] and Ag(100) [11] are very similar, except for the existence of a stable Cu monolayer phase on Au(100) [12,13]. With scanning tunneling microscopy (STM), it has been shown that the growth is layer-by-layer (<10 ML) [12]. The atomic distances, square symmetry, and the very smooth finish strongly support the formation of a pseudomorphic film [12,14]. This atomic arrangement, along with the measured step height, produces a structure which is close to bcc. For thicker films, a modulated structure aligned along the principal [100] and [001] directions appears [12] with a wavelength of about 60 Å and a height amplitude of 2 Å. Our x-ray scattering studies show conclusively that the height modulation which occurs at higher coverages originates from a restructuring of the entire film. We postulate a real space model of staggered, orthorhombic domains.

The x-ray scattering measurements were carried out at beam line X22A at the NSLS at Brookhaven National Laboratory using a four-circle goniometer at $\lambda = 1.20$ Å. Following convention, we use the tetragonal Au lattice parameters, $a = b = a_{\mathrm{Au}}$, and $c = \sqrt{2}\, a_{\mathrm{Au}}$ to define reciprocal space coordinates where the surface normal is along (001) [2]. The crystal was prepared in a multistep process including mechanical polishing, electropolishing,

 0031-9007/99/83(4)/780(4)$15.00

flame annealing, and electrochemical annealing to remove the islands which form after the lifting of the reconstructed phase. A thin (4μ) plastic window encapsulates the crystal in the x-ray electrochemical cell. The film was electrodeposited from a reservoir containing 0.1 M H_2SO_4 and 1 mM $CuSO_4$ [14] in the thick electrolyte regime. The copper film thickness was controlled by varying the deposition time (between 10 and 200 sec) at a potential of -0.3 V vs Ag/AgCl [14]. Prior to collecting x-ray data the cell was deflated leaving behind a thin electrolyte layer on the surface.

A schematic map of the main diffraction features is shown in Fig. 1 for the H-L plane. The positions and intensity distribution, by comparisons with real space models, provide detailed information on the atomic arrangement of the Cu and the Au near the surface. The unreconstructed Au(100) surface, both Cu free and with a pseudomorphic adlayer, gives rise to truncation rods (including the specular axis) where the intensity is simply related to a sum over atomic layers [15]. The formation of the modulated phase, occurring after the deposition of the 11th Cu layer, is accompanied by the simultaneous splitting of the specular quasi-Bragg peak and the appearance of satellite peaks displaced by multiples of a wave vector δ, along either $\langle 1,0,0\rangle$ (shown in Fig. 1) or $\langle 0,1,0\rangle$. For the thinnest films, $\delta = 0.049$ corresponds to a real space period $a_{\mathrm{Au}}/\delta = 59$ Å, in good agreement with the 62 Å reported with STM measurements [12]. Further Cu deposition did not change the essential nature of diffraction, suggesting that the underlying structural changes associated with the buckled phase are stable over a range of coverages. The modulation wave vector decreases from 0.049 to 0.040 (72 Å) as the thickness varied from 11 ML to ≈20 ML. Beyond about 20 ML, the appearance of powder $(1,1,1)_{\mathrm{fcc}}$ rings signified the formation of bulk Cu.

Figure 2 shows the specular reflectivity from the Au(100) surface with (*a*) no Cu, (*b*) a pseudomorphic Cu film with 7 layers, and (*c*) a modulated bcc Cu film with about 15 layers. The diffuse background, measured at displaced $H = 0.03$, has been subtracted from the data. The specular peak at $L = 2$ results from the underlying Au(001) planes. With no Cu, the reflectivity is in good agreement with the model curve (dashed line) for the ideally terminated Au lattice. The quasi-Bragg peak in 2(*b*) at $L \approx 2.8$ in the pseudomorphic phase signifies the existence of a finite number of Cu layers with a layer spacing ($2c/2.8$) differing from that of the underlying Au [14]. Analysis of the reflectivity in terms of a simple real space model [14] (solid line) yields a layer spacing of 1.45 ± 0.02 Å ($c/a = 1.00$). In the modulated phase, the peak at $L = 2.8$ found at lower coverages has symmetrically split into peaks at $L = 2.57$ and 3.07, as shown in 2(*c*). These two peaks suggest the formation of vertically expanded ($c = 1.59$ Å) and contracted ($c = 1.33$ Å) regions which accompanies the lateral modulation discussed above. Additional diffraction features close to the

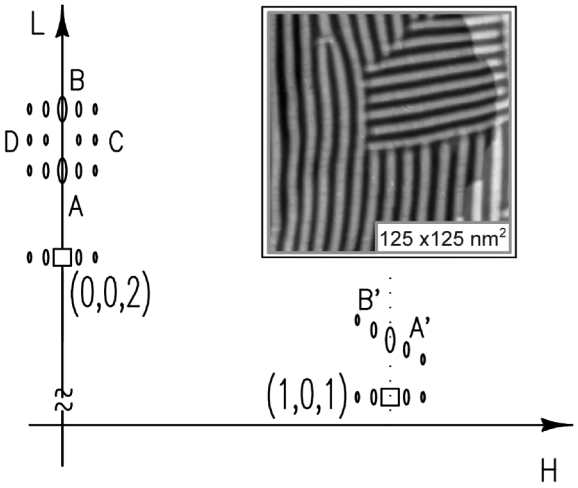

FIG. 1. The reciprocal space diffraction pattern in the (H, L) plane. The ellipses, scaled approximately with the intensity, correspond to the positions of diffraction peaks for Cu on Au(100) in the buckled phase. Inset: *In situ* STM image, under similar deposition conditions, exhibits a buckled texture.

specular axis further elucidate the nature of the modulated phase. Along $(\delta = 0.047, 0, L)$ [Fig. 1(*d*)], peaks are observed at $L = 2.0$, 2.61, and 3.03.

Insight into the nature of the relaxations which accompany the buckled phase is obtained from the scattering distribution at off-axis reciprocal space positions far from the specular axis. In Fig. 3(a) we show the scattered intensity (background subtracted) in the H-L plane close to $(1, 0, 1.4)$. Figure 3(b) shows scattering along the solid line Fig. 3(a). New diffraction peaks appear at $(0.92, 0, 1.51)$, $(0.96, 0, 1.45)$, $(1.04, 0, 1.32)$, and $(1.08, 0, 1.28)$. These four modulation peaks lie close to an arc of constant $|q| = 3.06 \pm 0.01$ Å^{-1}, shown by the dashed line in the figure. This $|q|$ is slightly larger than the corresponding value for the (111) fcc planes of Cu,

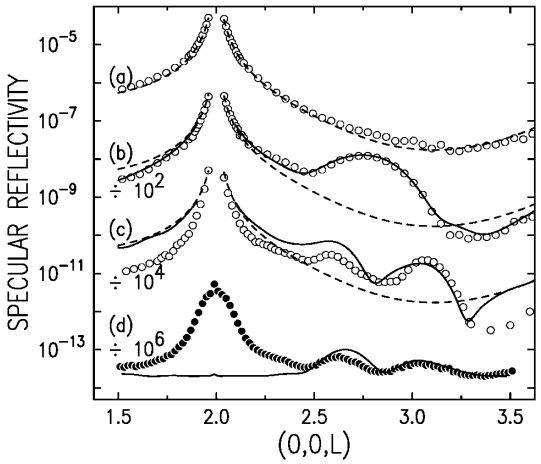

FIG. 2. X-ray reflectivity from the Au(100) surface in (*a*) the absence of Cu, (*b*) with 7.1 Cu layers, and (*c*) with about 14 Cu layers. In (*d*) the off-axis L scan $(\delta, 0, L)$ corresponds to the same film shown in (*c*). The dashed line is for an ideally terminated Au surface and the solid lines are the calculated model curves discussed in the text.

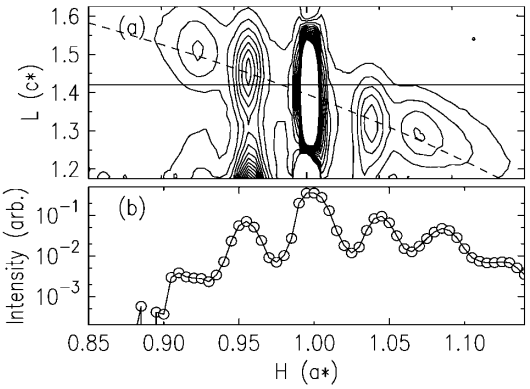

FIG. 3. (a) Equal intensity x-ray scattering contours near $(1, 0, 1.4)$. (b) $(H, 0, 1.4)$ scan. For both scans the intensity difference was calculated from measurements in the staggered orthorhombic phase and in a potential regime where no Cu is adsorbed.

3.01 Å^{-1}, and smaller than the expected value of 3.10 Å^{-1} for bcc Cu (assuming volume conservation). The arc of constant $|q|$ is suggestive of shearlike distortions of the film or a rotation. The diffraction widths along L are directly related to the number of Cu layers participating in the restructuring. The modulation peaks at $(\delta, 0, 2.61)$ and $(\delta, 0, 3.03)$, see Fig. 2(d), exhibit a peak width, $\Delta L = 0.11$ (rlu) FWHM. This is consistent with a film thickness, $0.9 \times \pi/(c^*\Delta L) = 16.7$ Å, or about 11.5 Cu layers. Similar widths are also obtained along the specular axis. The peaks at positions A' and B' (see Fig. 1) all have L widths close to 0.10 (rlu) FWHM. The thickness obtained from all of the L widths is close to the critical thickness (11 layers) where the buckled phase forms. Finally, there are no additional diffraction features transverse to the modulation vector, thus indicating the buckled Cu film is uniaxially commensurate along $\langle 0, 1, 0 \rangle$.

Several features in the diffraction pattern suggest that the buckled Cu induces a buckling in the underlying Au. These include the diffraction peaks at $(\delta, 0, 2)$, shown in Fig. 2(*d*), and at $(\pm\delta, 0, 1)$ and $(1 \pm \delta, 1, 1)$. At $(\delta, 0, 2)$, the profile appears Lorentzian with a width, $\Delta L = 0.1$ (rlu) FWHM. This suggests a surface induced distortion of the Au with a 13 Å exponential decay length, a distance very close to the calculated length of $a_{\text{Au}}/2\pi\delta = 11$ Å based on elasticity theory. Further confirmation of the buckling of the underlying Au is provided by the decrease in the wings of the reflectivity close to the (002) Bragg peak [Fig. 2(*c*)] which accompanies the formation of the buckled phase.

The diffraction features place stringent requirements on real space models. An approximate unit cell, $(24 \times 2 \times 6.5)$, is obtained from $1/\delta$ and the L widths. If the expanded and contracted regions, found in the specular data and denoted A and B in Fig. 1, conserve unit cell volume, then corresponding in-plane distortions are needed. We identify these with satellite peaks A' (associated with A) and B' (associated with B). Based on the position of the split peaks (on and off axis close to A and B), these regions should have a c/a ratio between 1.16 and 1.20. All of these peaks are modulated into discrete satellites with the spacing δ because of the formation of a regular striped structure. Finally the peaks C and D must be explained by additional rotated regions that remain approximately bcc. These bcc regions also contribute significantly to the off-axis scattering at A' and B'. A uniform expansion (compression), often observed in monolayer systems, would favor the A' (B') peaks and this is not observed.

The four regions attributed to the sets of peaks *A*-*D* can be seamlessly combined into the structure shown in Fig. 4. Solid lines are used to separate regions labeled *A*-*D* that give rise to peaks *A*-*D* following the same notation. A single parameter, representing the c/a ratio of the orthorhombic domains, has been adjusted to agree with the observed peak positions. Using the average $c/a = 1.18 \pm 0.03$, the predicted height modulation at the surface for the staggered model is $6(1.18 - 1.18^{-1}) \times 1.44$ Å $= 2.87$ Å, slightly larger than the value of 2 Å obtained with STM [12].

An important feature of this model is that it contains no dislocations within the Cu film, since all boundaries between domains [solid lines in Fig. 4(a)] lie along the $\{1, 0, 1\}$ bcc planes, reminiscent of martensitic distortions in bcc solids [3]. Note that these $\{1, 0, 1\}$ planes, which exhibit a quasihexagonal packing, are the close-packed bcc faces with the least corrugation, and hence can be most readily sheared.

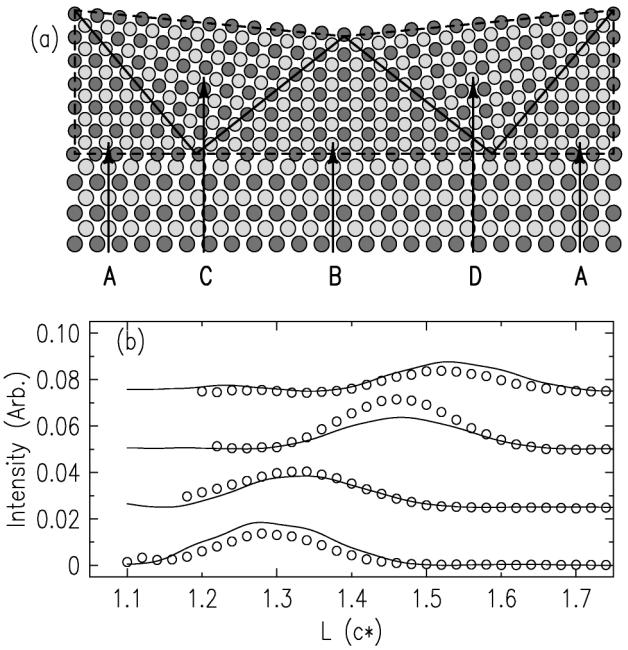

FIG. 4. (a) The proposed 2D atomic arrangement of the staggered orthorhombic phase for a $(24 \times 2 \times 6.5)$ slab. Regions A and B are orthorhombic and C and D are cubic. Every other row is displaced by 0.5 out of the plane. (b) L scans (open circles) through the four peaks shown by the contour plot in Fig. 3. The scattered intensity originating from the buckled Au layers has been subtracted. The staggered orthorhombic model results are drawn as solid lines.

The staggered orthorhombic model is compared with the x-ray scattering data with $c/a = 1.18$. We show the calculated scattering profiles at $(0, 0, L)$ and $(\delta, 0, L)$ in Figs. 2(*c*) and 2(*d*), respectively, as solid lines. The agreement for the $(\delta, 0, L)$ scan for the peak position, width, and amplitude provides support for the underlying features of the model. However, the specular data, which is sensitive to the strong interference with the underlying substrate, shows only moderate agreement (see below). The scattering near the $(1, 0, 1)$ peaks, shown in Figs. 3 and 4(b), provides further support for the model. At these positions, the model correctly predicts the peak widths and positions. Together, the diffraction data support $c/a = 1.18 \pm 0.03$.

Based on the staggered orthorhombic model motif, we have developed improved Cu models (not shown) [16]. The agreement with the specular reflectivity is significantly enhanced by including different Cu-Au layer spacings for regions *A* and *B* (see Fig. 4) and by incorporating the buckling of the underlying Au layers with an exponential decay length of 13 Å with a 0.1 Å amplitude [16]. The latter, with no adjustable parameters correctly describes the peak at $(\delta, 0, 2)$. Finally, more advanced models should also include interface alloying, a phenomenon observed in the STM stripping measurements [14], a spatial dependent c/a ratio, and a variable rms Debye-Waller amplitude. These are beyond the scope of the present paper [16].

First-principles full-potential calculations of the energies for orthorhombic Cu (not previously reported) are shown in Fig. 5. In each curve, b was fixed and for each c/a point the volume was relaxed (corresponding to $P = 0$) and the energy was calculated [2]. Here $b = a_{\mathrm{Au}}$ corresponds to the measured commensurate lattice along the $\langle 0, 1, 0 \rangle$ direction and $b = 1.02 \times a_{\mathrm{Au}}$ corresponds to a local-density-approximation calculation at $T = 0$ for Cu and Au. For all three curves, points with $c/a = 1$ are on the Bain path close to the bcc phase and the calculated energy is found to be close to 38 meV/atom greater than for fcc Cu. For $b = a_{\mathrm{Au}}$, minima are observed at $c/a = 1$ and $c/a \approx 1.22$. With decreasing b, the minimum decreases in energy and the corresponding c/a ratio increases. Fcc Cu corresponds to $b = a_{\mathrm{Au}}/1.129$ and $c/a = \sqrt{2}$ or, equivalently, for $b = \sqrt{2}\, a_{\mathrm{Au}}/1.129$ and $c/a = 1$. For each curve, the minimum c/a ratio is slightly larger than the measured value of 1.18, and the discrepancy may result from the absence of substrate interactions in the calculation. These findings clearly show that the "clamped" Cu phase is unstable with respect to an orthorhombic distortion.

Our study clearly establishes that the electrodeposition of Cu on Au(100) leads to an instability, analogous to a soft mode. At a critical thickness, the nearly bcc film formed at lower coverages forms a martensite-like microstructure composed of staggered, orthorhombic domains with $c/a = 1.18 \pm 0.03$. First-principles predictions, in the absence of surface terms, support the distortion with a slightly larger c/a ratio. Similar measurements on Au(100) and Ag(100) with vacuum phase deposition would help to provide a more complete description of this unusual buckled surface phase. Under these conditions it may also be possible to induce this "soft-mode" buckling with temperature at fixed coverages.

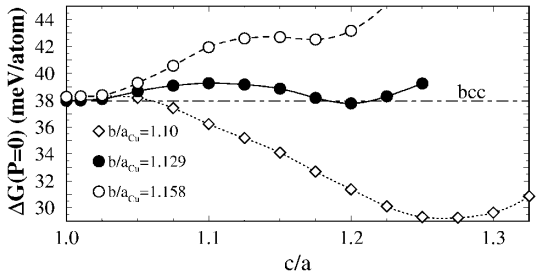

FIG. 5. First-principles full-potential calculations of the energies for orthorhombic Cu. In each curve, b was held fixed while c/a was varied.

BNL and the University of Illinois are supported by DOE Grants No. DE-AC-02-98CH10886 and No. DEFG02-96ER45439, respectively. This work is supported by the Deutsche Forschungsgemeinschaft through Graduiertenkolleg Nr. 328 "Molekulare Organisation an Grenz- und Oberflaechen."

[1] E. C. Bain, Trans. AIME **70**, 25 (1924).
[2] Throughout this paper, the lattice parameters a, b, a_{Cu}, and a_{Au} refer to nearest neighbor atomic spacings of the primitive unit cell, rather than the conventional cubic fcc cell.
[3] Z. Nishiyama, *Martensitic Transformations* (Academic Press, New York, 1978).
[4] Z. W. Lu, S.-H. Wei, and A. Zunger, Phys. Rev. B **41**, 2699 (1990).
[5] T. Kraft, P. M. Marcus, M. Methfessel, and M. Scheffler, Phys. Rev. B **48**, 5886 (1993).
[6] P. J. Craievich, M. Weinert, J. M. Sanchez, and R. E. Watson, Phys. Rev. Lett. **72**, 3076 (1994).
[7] E. Hahn, E. Kampshoff, N. Walchli, and K. Kern, Phys. Rev. Lett. **74**, 1803 (1995); F. B. Rasmussen, J. Baker, M. Nielsen, R. Feidenhans'l, and R. L. Johnson, Phys. Rev. Lett. **79**, 4413 (1997).
[8] R. Bruinsma and A. Zangwill, J. Phys. (Paris) **47**, 2055 (1986).
[9] L. A. Bruce and H. Jaeger, Philos. Mag. **36**, 1331 (1977).
[10] W. F. Egelhoff and I. Jacob, Phys. Rev. Lett. **62**, 921 (1989); W. F. Egelhoff, I. Jacob, J. M. Rudd, J. F. Cochran, and B. Heinrich, J. Vac. Sci. Technol. A **8**, 1582 (1990).
[11] M. Dietterle, T. Will, and D. M. Kolb, Surf. Sci. **396**, 189 (1998).
[12] R. J. Randler, M. Dietterle, and D. M. Kolb, Z. Phys. Chem. **208**, 43 (1999).
[13] M. Cappadonia, K. M. Robinson, J. Schmidberger, and U. Stimming, J. Electroanal. Chem. **436**, 73 (1997).
[14] R. J. Randler, D. M. Kolb, B. M. Ocko, and I. K. Robinson (to be published).
[15] I. K. Robinson and D. J. Tweet, Rep. Prog. Phys. **55**, 599 (1992).
[16] R. J. Randler, D. M. Kolb, B. M. Ocko, and I. K. Robinson (unpublished).